Published in final edited form as:
Brain Res. 2007 October 24; 1176: 45–52.

Neurochemical organization of the nucleus paramedianus dorsalis in the human

Joan S. Baizer[1], **James F. Baker**[2], **Kristin Haas**[1], and **Raquel Lima**[1]

1 *Department of Physiology and Biophysics, 123 Sherman Hall, University at Buffalo, State University of New York, Buffalo New York, 14214, phone: 716-829-3096, FAX: 716-829-2344, email: baizer@buffalo.edu*

2 *Department of Physiology, Institute for Neuroscience, Physiology/Medical, Ward 5-071, M211, Northwestern University Medical School, 303 East Chicago Avenue, Chicago, ILL 60611-3008*

Abstract

We have characterized the neurochemical organization of a small brainstem nucleus in the human brain, the nucleus paramedianus dorsalis (PMD). PMD is located adjacent and medial to the nucleus prepositus hypoglossi (PH) in the dorsal medulla, and is distinguished by the pattern of immunoreactivity of cells and fibers to several markers including calcium-binding proteins, a synthetic enzyme for nitric oxide (neuronal nitric oxide synthase, nNOS) and a nonphosphorylated neurofilament protein (antibody SMI-32). In transverse sections, PMD is oval with its long axis aligned with the dorsal border of the brainstem. We identified PMD in eight human brainstems, but found some variability both in its cross-sectional area and in its AP extent among cases. It includes calretinin immunoreactive large cells with oval or polygonal cell bodies. Cells in PMD are not immunoreactive for either calbindin or parvalbumin, but a few fibers immunoreactive to each protein are found within its central region. Cells in PMD are also immunoreactive to nNOS, and immunoreactivity to a neurofilament protein shows many labeled cells and fibers. No similar region is identified in atlases of the cat, mouse, rat or monkey brain, nor does immunoreactivity to any of the markers that delineate it in the human reveal a comparable region in those species. The territory that PMD occupies is included in PH in other species. Since anatomical and physiological data in animals suggest that PH may have multiple subregions, we suggest that the PMD in human may be a further differentiation of PH, and may have functions related to the vestibular control of eye movements.

Keywords

eye movements; nucleus prepositus hypoglossi; calretinin; calbindin; parvalbumin; cerebellum; nitric oxide; vestibular nuclear complex

INTRODUCTION

The human brain is larger and has a more complex organization than the brains of lower mammals, including nonhuman primates. However, the majority of studies on human brain organization are concerned with the cerebral cortex, with the tacit assumption that the organization of the "older" brainstem is much more conserved across species. We have been studying the neurochemical organization of the vestibular nuclear complex of the brainstem in

Correspondence to: Joan S. Baizer.

animals (Baizer and Baker, 2005; Baizer and Baker, 2006a; Baizer and Baker, 2006b), and have recently begun extending this analysis to the human brain (Baizer et al., 2006). In the human, we noticed a dense cluster of calretinin immunoreactive cells in an oval region at the anterior-posterior (A-P) level of, but medial to, the nucleus prepositus hypoglossi (PH). This region corresponds to the nucleus paramedianus dorsalis identified from Nissl sections (Olszewski and Baxter, 1954; Sadjadpour and Brodal, 1968; Paxinos and Huang, 1995). It is darkly stained and better visualized in sections stained for acetylcholinesterase (Paxinos and Huang, 1995). We have studied the neurochemical organization of this nucleus using immunohistochemical techniques and antibodies to several markers that have been useful in delineating compartments or cell populations in other locations in the brain. These included the calcium-binding proteins, which mark inhibitory neurons in the cerebral and cerebellar cortex (Arai et al., 1991; Celio, 1990), the synthetic enzyme for nitric oxide, nNOS, which is found in cell populations in the nucleus prepositus hypoglossi (PH; Moreno-López et al., 2001; Moreno-Lopez et al., 1998; Van Brederode, et al., 1990) and a nonphosphorylated neurofilament protein which labels a subset of pyramidal cells in the cerebral cortex (Hof et al., 1990; Hof and Morrison, 1990). We suggest that PMD may be a phylogenetically “new” nucleus present in humans and possibly in great apes as well.

RESULTS

Organization of the human medulla; location of PMD

We compared our sections to the illustrations of transverse sections of the human brainstem (Olszewski and Baxter, 1954) to identify structures. The extent of the human medulla and pons in the A-P direction is about 40 mm. The vestibular nuclear complex (VNC) is present over about 12 mm, and the nucleus prepositus hypoglossi (PH) over about 6 mm. Figure 1 shows the structures of the medulla at the caudal (Fig. 1A) and rostral (Fig. 1B) limits of PMD. The organization of the caudal human medulla is strikingly different from that of cat (see Berman, 1968) or monkey (see Paxinos et al.. 2000) in that it is expanded ventrolaterally to encompass the very much enlarged inferior olive (Fig. 1A). The nucleus paramedianus dorsalis (PMD) begins at about the same A-P level as PH, just rostral to the hypoglossal nucleus. Figure 2 shows PMD from one of our cases on a section stained with cresyl violet. At the lower magnification view, (Fig. 2A) PMD is seen bilaterally as an oval cluster of large cells, with the dorsal edge of the brainstem curved around it (Fig. 2A, arrows). The long axis of PMD on this section is about 800 μm and the short axis about 400 μm (Fig. 2A). It is set off from the more lightly stained reticular formation ventrally and PH laterally. The cells in this region have large oval or polygonal cell bodies (Fig. 2B, arrows) that stain darkly with a Nissl stain.

Calcium-binding proteins in PMD

PMD is much more prominent in sections processed for calretinin immunoreactivity than in Nissl-stained sections. Figure 3A (arrow) shows that PMD is more darkly stained for calretinin immunoreactivity than the reticular formation ventrally and PH laterally. At a higher magnification (Fig. 3B) it is apparent that this dark staining in PMD reflects the many large somas and proximal processes that are strongly immunoreactive to calretinin. The appearance of PMD in sections processed for calbindin immunoreactivity is quite different. Figure 4A shows that there are no cells in PMD that are immunoreactive to calbindin, in contrast to the darkly stained cells and processes in the reticular formation just ventral to it (Fig. 4A, arrowhead; Fig. 4B, arrow). The center region of PMD has fine, varicose calbindin immunoreactive fibers (Fig. 4B, C). Fig. 4A also illustrates darker patches of calbindin label more laterally in the section (Fig. 4A, arrows). The overall pattern of calretinin and calbindin label in the human VNC will be the subject of a subsequent report.

The appearance of the region in sections processed for parvalbumin reactivity is different yet again. Figure 5A shows dark staining in much of the dorsal and lateral brainstem, with several darkly stained patches (Fig. 5A, white arrowheads). The staining in PH is lighter than the staining lateral to it, and PMD is distinct since the region looks white in contrast to the region around it (Fig. 5A, arrow). Within PMD, however, are stained fine varicose fibers (Fig. 5B) that are quite similar to the calbindin immunoreactive fibers shown in Fig. 4C.

nNOS; SMI-32

We also looked at immunoreactivity for the synthetic enzyme for nitric oxide, nNOS, since previous studies have shown many cells in PH synthesize nitric oxide and are immunoreactive for this antibody (Baizer and Baker, 2006b; Moreno-López et al., 2001). Figure 6A (arrow) shows that PMD is very darkly stained with nNOS immunoreactivity. PH (Fig. 6A, region between the arrowheads) also has many immunoreactive cells. Figure 6B shows the sizes and spacing of nNOS immunoreactive cells in PMD. Cell bodies are round or polygonal, and the proximal processes are stained (Fig. 6B, examples at arrows).

Finally, we looked at the pattern of immunoreactivity to a neurofilament protein, using the antibody SMI-32. We had previously found subsets of cells in the VNC of both cat and monkey that were immunoreactive to this antibody (Baizer and Baker, 2004). Figure 7A shows that PMD is a clearly demarcated darkly-stained oval region in a section processed for SMI-32 immunoreactivity. Figure 7B is a higher magnification view of PMD, showing that this dark staining is comprised of somas and processes. The stained fibers are seen running in all orientations (Fig. 7C, arrows).

Variability of PMD among cases

Olszewski and Baxter (1954) note that the “degree of development (of PMD) …varies remarkably from one individual to another.” PMD was present in all eight cases we examined, but its size, both cross-sectional area and anterior-posterior extent, varied among cases. Figure 8 illustrates the variations in the size of PMD in four additional cases on sections at about the A-P center of PMD in each case. PMD appears greatly expanded in Case 164 compared to the other cases. PMD always began caudally at about the same location in the medulla, just rostral to the hypoglossal nucleus. In four of the eight cases (Cases 164, 169, Fig. 8, and Cases 155, 158, not shown), it continued rostrally to the level of the genu of the seventh nerve. The total A-P extent varied from about 5–8 mm.

DISCUSSION

We have described the neurochemical properties of cells and fibers in a small oval nucleus in the posterior medulla of the human brain. Following earlier terminology (Olszewski and Baxter, 1954; Paxinos and Huang, 1995) we are referring to this region as the nucleus paramedianus dorsalis, PMD. It is neurochemically distinct from the reticular formation ventral to it and the nucleus prepositus hypoglossi that is lateral to it. The inputs to and projections from this region are entirely unknown. Largely on the basis of the appearance of the cells, Olszewski and Baxter (1954) proposed that the nucleus “represents a group of caudally and dorsally displaced pontine nuclei which send their axons to the contralateral cerebellum.” This remains an untested hypothesis; the tracer Di-I that transports in fixed tissue (review in Sparks et al., 2000) could be used to determine the connections of PMD in the human. The presence of acetylcholinesterase staining (Paxinos and Huang, 1995) suggests cholinergic input; data from animals suggest that possible sources of this input are the vestibular nuclei or PH (Barmack et al., 1992).

How do our data compare with other descriptions of PMD? We estimated the A-P extent of PMD as about 5–8 mm. The A-P extent calculated the sections shown in the atlases is about 4 mm (Olszewski and Baxter, 1954; Paxinos and Huang, 1995). In those atlases, PMD is divided into oral and caudal subdivisions (Olszewski and Baxter, 1954; Paxinos and Huang, 1995); in our sections it appeared as an uninterrupted cell column and we were unable to distinguish these subdivisions. There are two other differences between our material and the illustrations of PMD in those atlases. First, PMD is relatively larger in our sections, and, second, we see the dorsal brainstem curving gently over it. Since the illustrations in each atlas are based on a single case, these differences may be a further reflection of individual differences in the size and shape of PMD suggested by our eight cases.

What might be the function of PMD? Inferences about the function of components of the human brainstem are usually based on the anatomical and electrophysiological study of those structures in animals. In that context, this nucleus presents a challenge since it is not distinguished in atlases of the mouse (Franklin and Paxinos, 1997), rat (Paxinos and Watson, 1997), cat (Berman, 1968), squirrel monkey (Emmers and Akert, 1963), or rhesus monkey (Paxinos et al., 2000). In those atlases, the region in which PMD is found is included in PH. Brodal (1983) did note that a region similar to PMD as described in humans was “discernible but less distinct also in the monkey and the chimpanzee.” However, this was a comment in the Discussion; he did not illustrate the cells in question for either species in that paper or in a subsequent study of monkey VNC (Brodal, 1984). We found that immunoreactivity to both calretinin and calbindin in PH of the monkey was uniform; there was no indication of a distinct oval region medial in PH (Baizer and Baker, 2006a, Fig. 4). Immunoreactivity to nNOS in the macaque monkey likewise did not reveal a cell group in the expected location of PMD (Baizer and Baker, 2006b, Fig. 9). We did find a small cluster of cells in PH of the monkey immunoreactive to a chondroitin sulfate proteoglycan that is labeled with an antibody called 8B3; this antibody labels a small set of cells at various sites in the brain (Baizer and Baker, 2006b; Pimenta et al., 2001 and unpublished observations). The location of the 8B3 immunoreactive cells is somewhat more lateral than the putative location of PMD (Baizer and Baker, 2006b, Fig. 8). We have not yet succeeded in getting good immunostaining with this antibody in the human material. However, the observation of a neurochemically distinct cell cluster in PH is consistent with the idea that there are multiple functional subdivisions of this nucleus. This idea is further supported by studies in animals that show that different parts of PH have different connections (Klop et al., 2005; Langer et al., 1986).

One very tentative interpretation of the present data then, is that the PMD is part of PH in the animals studied so far, but in humans is a separate nucleus. If this were true, its functions might be aligned to those of PH, receiving vestibular input and participating in the control of eye movements (Belknap and McCrea, 1988; Kaneko, 1992; Kaneko, 1997; Kaneko, 1999; McCrea and Baker, 1985; McCrea et al., 1979). While the eye movements of humans and monkeys are very similar, some subtle differences have been described (Baizer and Bender, 1989). Verifying this idea may have to await either the development of much greater accuracy in imaging methods or tract tracing studies in fixed tissue (Sparks et al., 2000). The differences among cases in the size of PMD, then, might correlate with individual differences in oculomotor performance; unfortunately there are no data about the oculomotor abilities of these cases. It would also be of interest to examine the brainstems of great apes to see if the nucleus is present in any nonhuman primates.

Experimental Procedures

METHODS

We studied eight brainstems from the Witelson Normal Brain Collection (Witelson and McCulloch 1991). The brains had been stored in 10 % formalin. The brainstems were dissected

away from the brain and a slit made down the ventral surface on the right side to allow identification of right and left sides of the brainstem on sections. The brainstems were then cryoprotected in 15% and then 30% sucrose formalin. Forty μm frozen sections were cut on a sliding microtome in the transverse plane, and stored in compartment boxes, 5 sections/compartment, in 5% formalin at 4° C. Initially, for each case, sets of sections about 2 mm apart through the brainstem were mounted on gelatin-coated glass slides and stained for cresyl violet (LaBossiere and Glickstein, 1976). Other sets of sections were processed for immunohistochemistry using techniques that are standard in this laboratory with the addition of an antigen retrieval (AR) protocol. Sections were rinsed in PBS and placed individually in glass jars in 20 cc of a solution of citric acid, pH adjusted to 8.0. They were then heated in a water bath to 85° for 20 minutes, cooled for 20 minutes, and the sections removed and rinsed in PBS before proceeding with the immunohistochemistry protocol. This AR protocol worked well for antibodies to the calcium-binding proteins and SMI-32. Immunostaining for nNOS was variable among cases. After the AR procedure, sections were incubated in a blocking solution of PBS with 4–5% nonfat dry milk or 1% Bovine Serum Albumin (Sigma), 2.0% Triton-X100, and 1.0–1.5% normal serum, (Vector Laboratories, Burlingame, CA). The primary antibody was added and sections were incubated overnight at 4° with gentle agitation. Table 1 shows the primary antibodies and dilutions used. Subsequent processing was with the appropriate Vector ABC Elite kit (mouse or rabbit). For some sections, immunoreactivity was visualized by incubating in 3, 3′-diaminobenzidine (DAB, Sigma) with 0.0015–0.003% H_2O_2 in 0.01M PBS. For other sections, immunoreactivity was visualized by the glucose oxidase (GO) modification of the DAB procedure (Shu et al., 1988). We found that the GO procedure decreased the nonspecific staining and allowed better visualization of axon terminals than the standard DAB procedure. The photomicrographs all show sections processed with the GO method. Images were captured with a Spot Insight Camera mounted on a Leitz Dialux 20 microscope. They were imported into Adobe Photoshop, contrast and brightness adjusted and plates assembled with that software. All images are shown as right side views for ease of comparison.

Acknowledgements

Supported by a subcontract from EY07342 (James F. Baker, PI). We are grateful to Sandra F. Witelson for the generous gift of brainstems from the Witelson Normal Brain collection, and to Debra L. Kigar for help in selecting cases and with the initial dissections.

References

Arai R, et al. Immunohistochemical localization of calretinin in the rat hindbrain. J Comp Neurol 1991;310:21–44. [PubMed: 1939729]

Baizer J, Baker J. Immunoreactivity for SMI-32 and CAT-301 in the vestibular nuclear complex of the cat. Neurosci Abs 2004:#652.615.

Baizer JS, Baker JF. Immunoreactivity for calcium-binding proteins defines subregions of the vestibular nuclear complex of the cat. Exp Brain Res 2005;164:78–91. [PubMed: 15662522]

Baizer JS, et al. Immunoreactivity for calretinin defines a subdivision of the medial vestibular nucleus in the human. Neurosci Abs 2006:#550.10.

Baizer JS, Baker JF. Immunoreactivity for calretinin and calbindin in the vestibular nuclear complex of the monkey. Exp Brain Res 2006a;172:103–13. [PubMed: 16369782]

Baizer JS, Baker JF. Neurochemically defined cell columns in the nucleus prepositus hypoglossi of the cat and monkey. Brain Res 2006b;1094:127–37. [PubMed: 16701575]

Baizer JS, Bender DB. Comparison of saccadic eye movements in humans and macaques to single-step and double-step target movements. Vision Res 1989;29:485–95. [PubMed: 2781737]

Barmack NH, et al. Cholinergic innervation of the cerebellum of the rat by secondary vestibular afferents. Ann N Y Acad Sci 1992;656:566–79. [PubMed: 1376098]

Belknap DB, McCrea RA. Anatomical connections of the prepositus and abducens nuclei in the squirrel monkey. J Comp Neurol 1988;268:13–28. [PubMed: 3346381]

Berman, A. The brain stem of the cat. University of Wisconsin Press: Madison, Wisconsin; 1968.

Brodal A. The perihypoglossal nuclei in the macaque monkey and the chimpanzee. J Comp Neurol 1983;218:257–69. [PubMed: 6886074]

Brodal A. The vestibular nuclei in the macaque monkey. J Comp Neurol 1984;227:252–66. [PubMed: 6470216]

Celio MR. Calbindin D-28k and parvalbumin in the rat nervous system. Neuroscience 1990;35:375–475. [PubMed: 2199841]

Emmers, R.; Akert, K. A stereotaxic atlas of the brain of the squirrel monkey (Saimiri sciureus). University of Wisconsin Press; Madison: 1963.

Franklin, KBJ.; Paxinos, G. The mouse brain in stereotaxic coordinates. Academic Press; San Diego: 1997.

Hof PR, et al. Quantitative analysis of a vulnerable subset of pyramidal neurons in Alzheimer's disease: I. Superior frontal and inferior temporal cortex. J Comp Neurol 1990;301:44–54. [PubMed: 2127598]

Hof PR, Morrison JH. Quantitative analysis of a vulnerable subset of pyramidal neurons in Alzheimer's disease: II. Primary and secondary visual cortex. J Comp Neurol 1990;301:55–64. [PubMed: 1706358]

Kaneko CR. Effects of ibotenic acid lesions of nucleus prepositus hypoglossi on optokinetic and vestibular eye movements in the alert, trained monkey. Ann N Y Acad Sci 1992;656:408–27. [PubMed: 1599159]

Kaneko CR. Eye movement deficits after ibotenic acid lesions of the nucleus prepositus hypoglossi in monkeys. I. Saccades and fixation. J Neurophysiol 1997;78:1753–68. [PubMed: 9325345]

Kaneko CR. Eye movement deficits following ibotenic acid lesions of the nucleus prepositus hypoglossi in monkeys II. Pursuit, vestibular, and optokinetic responses. J Neurophysiol 1999;81:668–81. [PubMed: 10036269]

Klop EM, et al. Two parts of the nucleus prepositus hypoglossi project to two different subdivisions of the dorsolateral periaqueductal gray in cat. J Comp Neurol 2005;492:303–22. [PubMed: 16217796]

LaBossiere, E.; Glickstein, M. Histological processing for the neural sciences. Charles C. Thomas; Springfield, Illinois: 1976.

Langer T, et al. Afferents to the abducens nucleus in the monkey and cat. J Comp Neurol 1986;245:379–400. [PubMed: 3082944]

McCrea RA, Baker R. Cytology and intrinsic organization of the perihypoglossal nuclei in the cat. J Comp Neurol 1985;237:360–76. [PubMed: 4044893]

McCrea RA, et al. Afferent and efferent organization of the prepositus hypoglossi nucleus. Prog Brain Res 1979;50:653–65. [PubMed: 551460]

Moreno-López B, et al. Morphological identification of nitric oxide sources and targets in the cat oculomotor system. J Comp Neurol 2001;435:311–24. [PubMed: 11406814]

Moreno-López B, et al. Mechanisms of action and targets of nitric oxide in the oculomotor system. J Neurosci 1998;18:10672–9. [PubMed: 9852602]

Olszewski, J.; Baxter, D. Cytoarchitecture of the human brain stem. Karger; Basel: 1954.

Paxinos, G.; Watson, C. The rat brain, in stereotaxic coordinates. Academic Press; San Diego: 1997.

Paxinos, G.; Huang, XF. Atlas of the human brainstem. Academic Press; San Diego: 1995.

Paxinos, G., et al. The rhesus monkey brain in stereotaxic coordinates. Academic Press; San Diego: 2000.

Pimenta AF, et al. Novel proteoglycan epitope expressed in functionally discrete patterns in primate cortical and subcortical regions. J Comp Neurol 2001;430:369–88. [PubMed: 11169474]

Sadjadpour K, Brodal A. The vestibular nuclei in man. A morphological study in the light of experimental findings in the cat. J Hirnforsch 1968;10:299–323. [PubMed: 5732949]

Shu SY, et al. The glucose oxidase-DAB-nickel method in peroxidase histochemistry of the nervous system. Neurosci Lett 1988;85:169–71. [PubMed: 3374833]

Sparks DL, et al. Neural tract tracing using Di-I: a review and a new method to make fast Di-I faster in human brain. J Neurosci Methods 2000;103:3–10. [PubMed: 11074091]

Van Brederode JF, et al. Calcium-binding proteins as markers for subpopulations of GABAergic neurons in monkey striate cortex. J Comp Neurol 1990;298:1–22. [PubMed: 2170466]

Witelson SF, McCulloch PB. Premortem and postmortem measurement to study structure with function: a human brain collection. Schizophr Bull 1991;17:583–91. [PubMed: 1805351]

Figure 1.

The organization of the human medulla at the caudal (A) and rostral (B) limits of the nucleus paramedianus (arrows). The two sections are about 4 mm apart. Adapted from plates drawn from Nissl sections in the atlas of Olszewski and Baxter (1954). Abbreviations: Am, nucleus ambiguus; Arc, nucleus arcuatus; Cor. po, Nucleus corporis pontobulbaris; Co. v, Nucleus cochlearis ventralis; Cu .l, nucleus cuneatus lateralis; D. mo. X, Nucleus dorsalis motorius nervi vagi; Gc, nucleus gigantocellularis; Ipo, Nucleus interpositus; Le. m, lemniscus medialis; N VII, Nucleus nervi facialis; Ol. i. d, Nucleus olivaris inferior accessorius dorsalis; Ol. i. m Nucleus olivaris inferior accessorius medialis; Ol. i. pr, Nucleus olivaris inferior principalis; Ov, Nucleus ovalis; Pc, nucleus parvocellularis; Pe. ce. i, Pedunculus cerebelli inferior; Pg. d, Nucleus paragigantocellularis dorsalis; Pg. l, Nucleus paragigantocellularis lateralis; Pm. c, Nucleus paramedianus dorsalis caudalis; Pm. o, Nucleus paramedianus dorsalis oralis; Prp, Nucleus prepositus hypoglossi; Pyr, pyramis; Ra. ob, Nucleus raphae obscurus; Ra. pa, Nucleus raphae pallidus; Sol, Nucleus tractus solitarii; Sp. V. o, Nucleus tractus spinalis trigemini oralis; St. gl, Stratum gliosum subependymale; Sub, Nucleus medullae oblongatae subtrigeminalis; T. sol, Tractus solitarius; T. sp. V, Tractus nervi trigemini spinalis; VIII. m, Nucleus vestibularis medialis; VIII. sp, Nucleus vestibularis spinalis; α Islands of cells that resemble cells on the pontine gray.

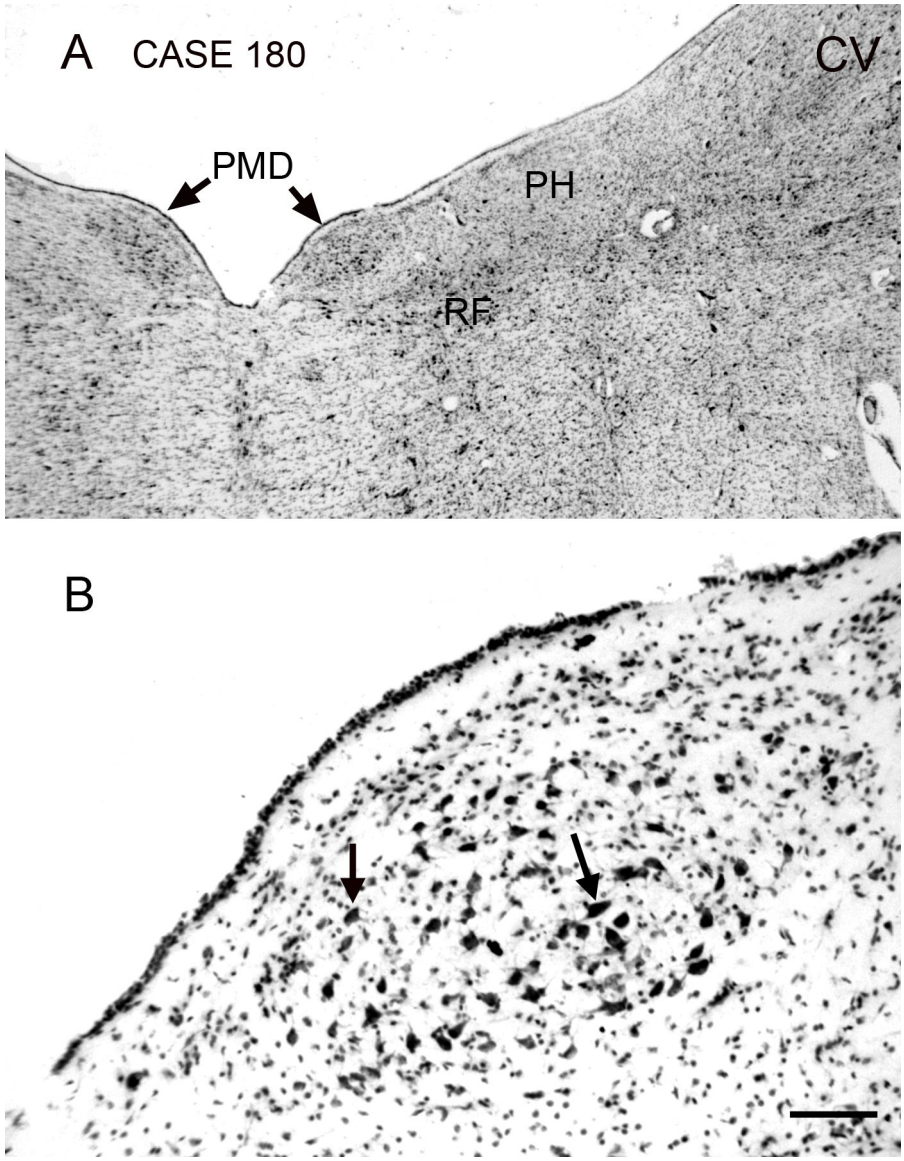

Figure 2.

The nucleus paramedianus dorsalis (PMD), Nissl staining, transverse section. The A-P extent of the nucleus in this case is about 5 mm. The section shown is about 2 mm rostral to the caudal pole of PMD. **A.** The arrows indicate PMD, which is seen as a darkly stained oval region lying just medial to the nucleus prepositus hypoglossi (PH), lateral to the midline and dorsal to the reticular formation (RF). Scale bar 1 mm. **B.** PMD consists of cells with large irregularly shaped somas; examples at arrows. Abbreviations: CV, cresyl violet; RF, reticular formation. Scale bar 100 μm. Case180, m, age 54.

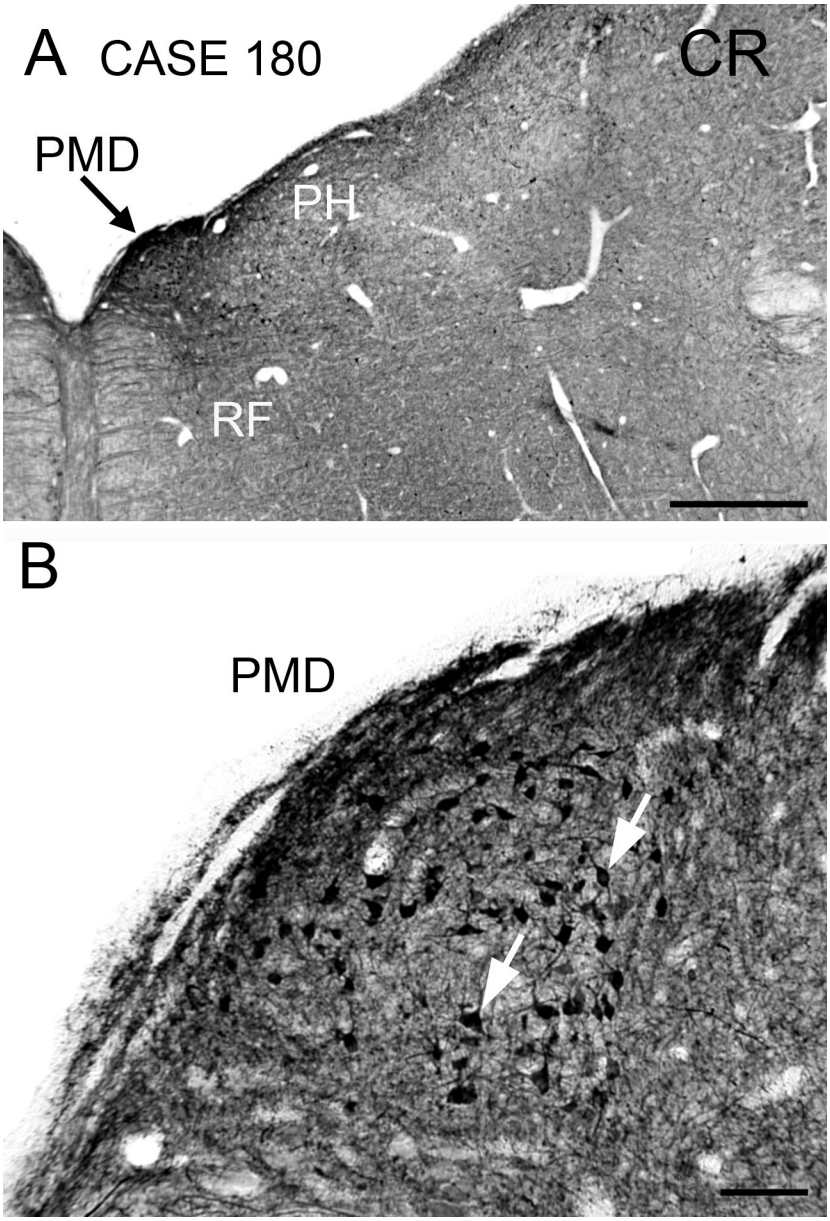

Figure 3.

Immunoreactivity to calretinin in PMD on a section at the same level as in Fig. 1. **A.** The arrow shows PMD, which is darkly stained in contrast to PH laterally and the midline reticular formation. Scale bar 1 mm. **B.** Calretinin immunoreactive cells in PMD (arrows) have oval or polygonal cell bodies. Abbreviation: CR, calretinin. Scale bar 100 μm.

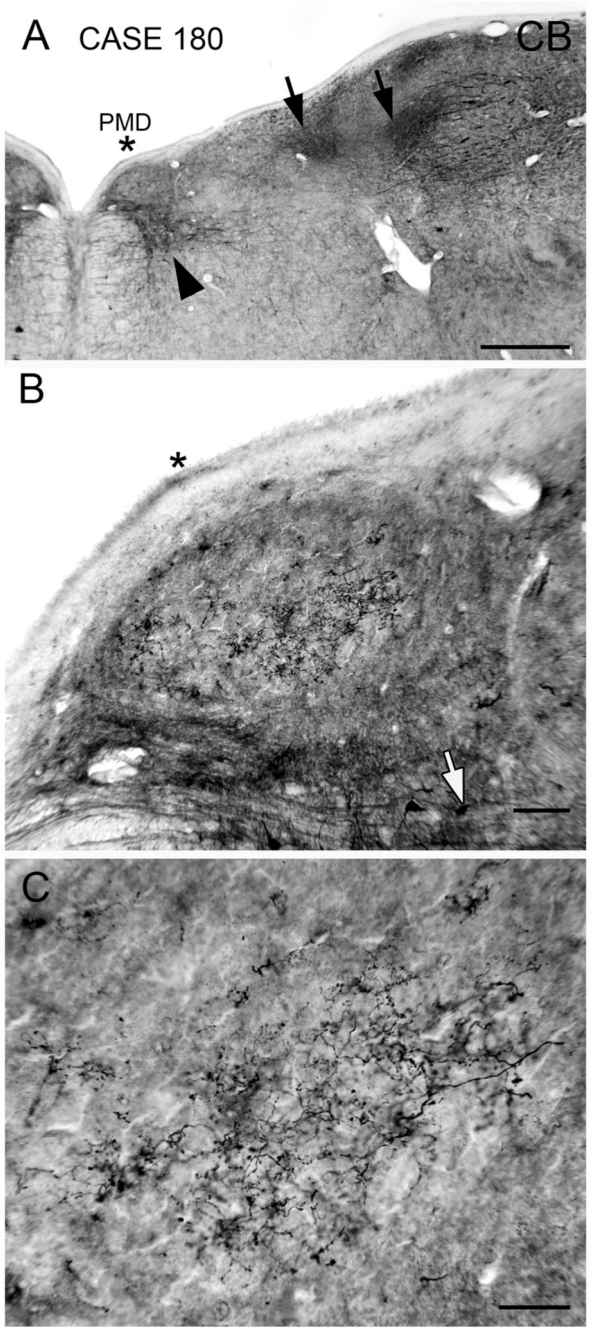

Figure 4.

Immunoreactivity to calbindin in PMD; section about 200 μm rostral to the one in Fig. 3. **A.** PMD is lightly stained and is located just dorsal to a darkly stained patch of cells and fibers in the reticular formation (black arrowhead). There are several darkly stained patches (arrows) more laterally. The asterisk is an alignment point. Scale bar 1 mm. **B.** Immunoreactive fine varicose fibers in the central part of PMD. The asterisk is at the same position as in A. Scale bar 100 μm. **C.** Higher magnification image of the calbindin immunoreactive varicose processes in the center of PMD. Abbreviations: CB, calbindin. Scale bar 50 μm.

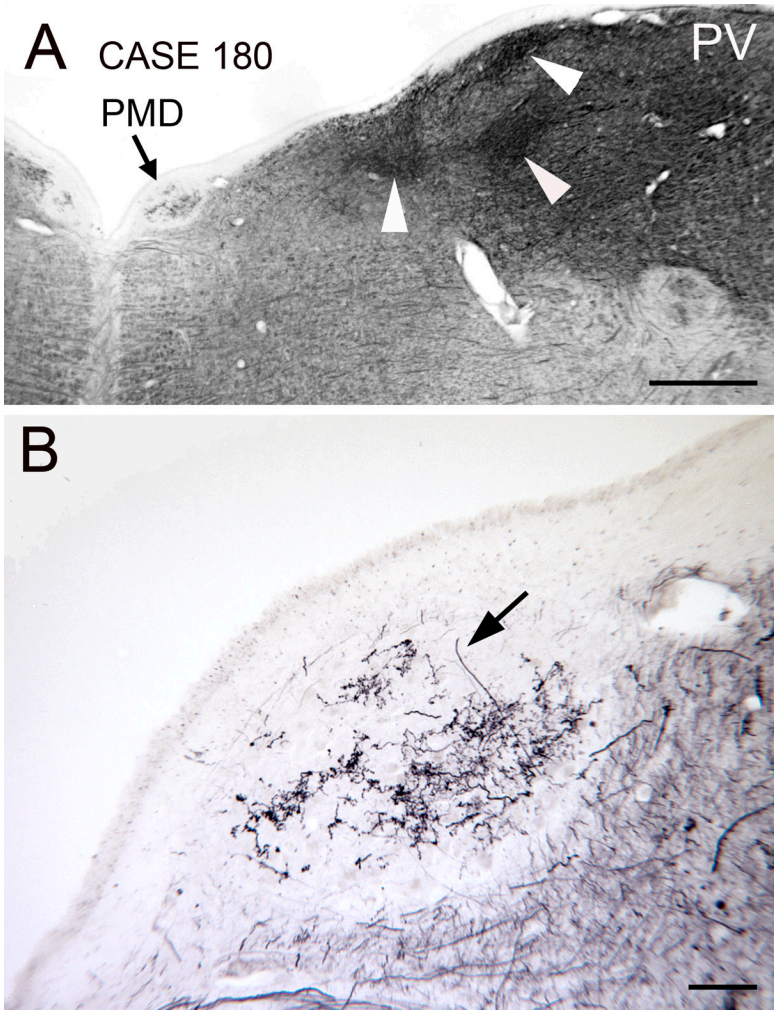

Figure 5.
Parvalbumin immunoreactivity in PMD. The section is about 1 mm rostral to the posterior pole of PMD. **A.** The arrow points to PMD which is seen as a white oval with some staining in the center. The arrowheads point to darker patches of parvalbumin immunoreactivity laterally in the dorsal brainstem. Scale bar 1 mm. **B.** Higher magnification view of the fiber staining in the center of PMD. The arrow indicates one immunoreactive fiber. Abbreviation: PV, parvalbumin. Scale bar 100 μm.

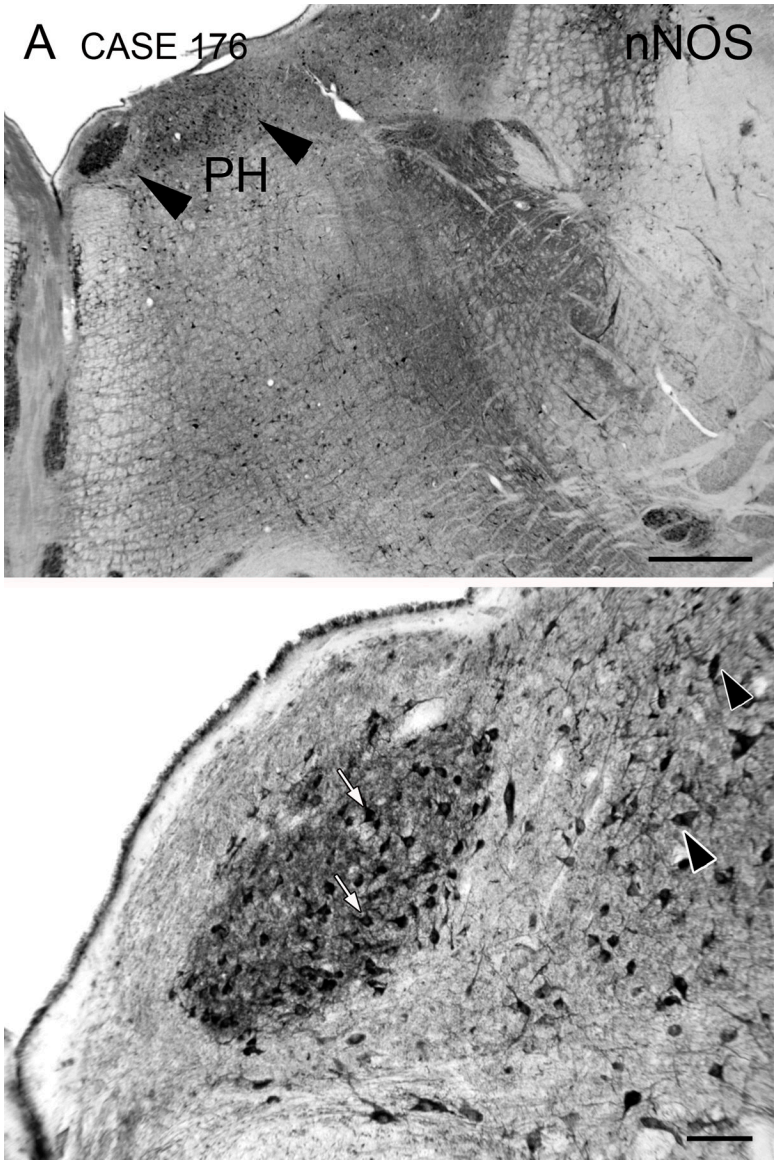

Figure 6.

Nitric oxide synthase (nNOS) immunoreactivity in PMD. **A.** PMD is a darkly stained oval, and is the most darkly stained structure in the dorsal brainstem. The arrowheads show the approximate medial and lateral borders of PH, in which stained cells are also seen. Scale bar 1 mm. **B.** Darkly stained cells (arrows) and neuropil in PMD. The arrowheads indicate stained cells in PH. Scale bar 100 μm. The A-P extent of PMD is about 6 mm. The section illustrated is about 200 μm rostral to its posterior pole. Case 176, f, age 71.

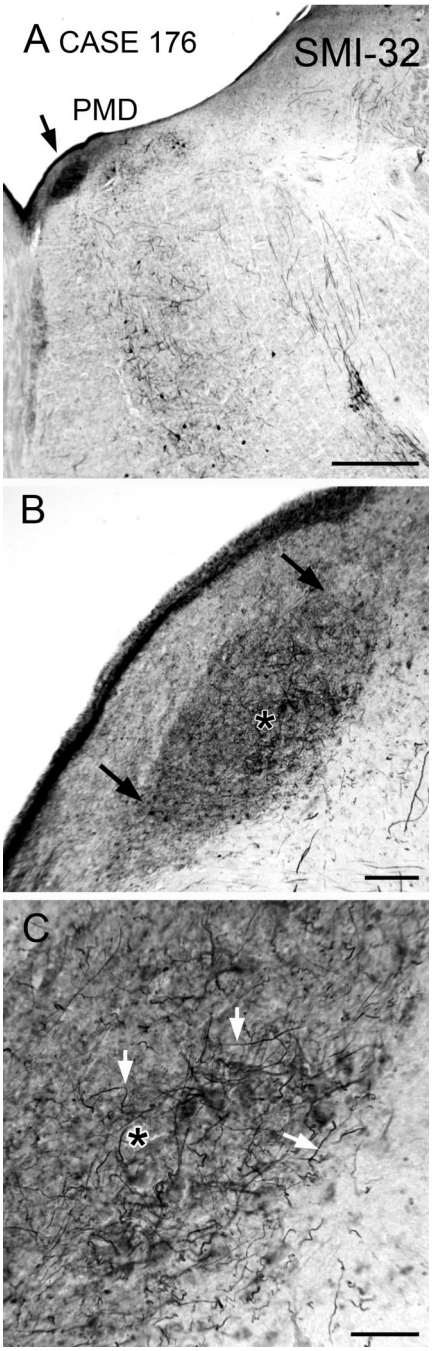

Figure 7.
Immunoreactivity to a nonphosphorylated neurofilament protein in PMD on a section close to the caudal pole. **A.** Arrow shows the location of PMD, a dark oval. Scale bar 1 mm. **B.** Higher magnification image of PMD; arrows indicate its borders. The asterisk is an alignment point for C. Scale bar 100 μm. **C.** Stained fibers in PMD (examples at arrows) running in all directions on a background of darkly-stained neuropil. Asterisk as in B. Abbreviation: SMI-32, antibody to neurofilament protein. Scale bar 50 μm.

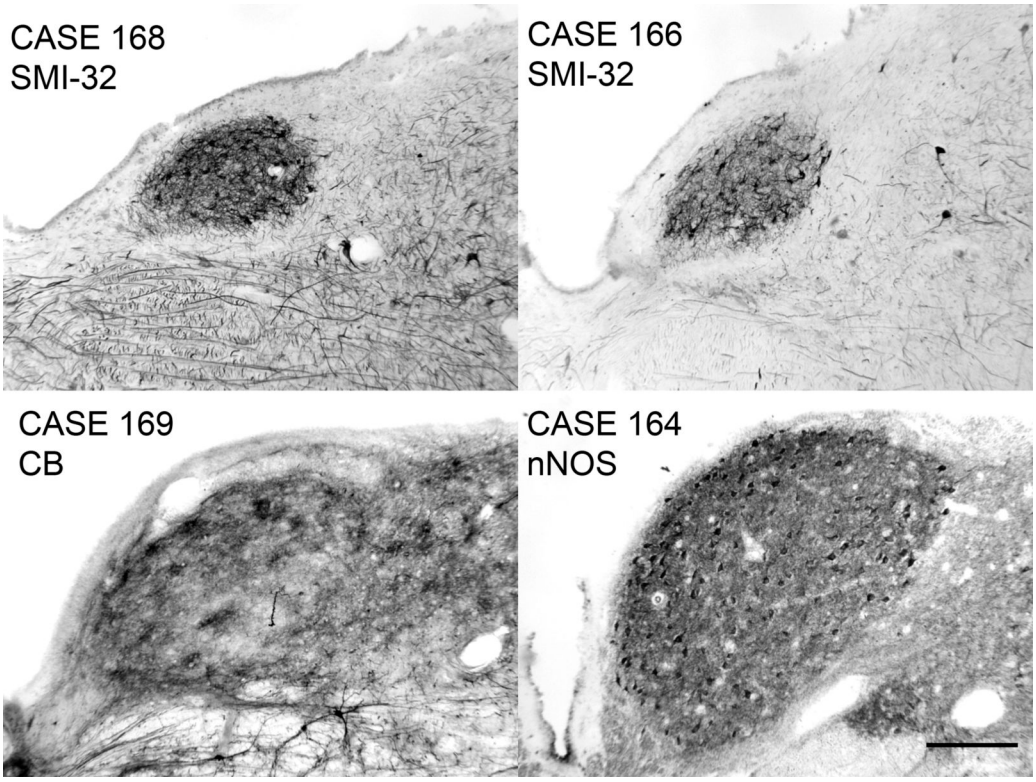

Figure 8.
Variability of the size and shape of PMD in four cases. The sections are at about the A-P center of PMD. Case 168, m, age 69, A-P extent of PMD about 6 mm. Case 166, f, age 75. A-P extent about 5 mm. Case 169, m, age 70, A-P extent about 7 mm. Case 164, f, age 45; A-P extent about 8 mm. Scale bar (for all panels) 250 μm.

TABLE 1

Antibodies and dilutions.

antibody	source	dilution
calbindin	Chemicon AB1778	1:1000
calretinin	Chemicon AB5054	1:1500
calretinin	Chemicon MAB1568	1:500–1:1000
nNOS	Cayman Chemical 160870	1:200–1:300
parvalbumin	Sigma P3171	1:2000
SMI-32	Sternberger Monoclonals SMI 32	1:1500